From Homogeneous Electroenzymatic Kinetics to Antigen−Antibody Construction and Characterization of Spatially Ordered Catalytic Enzyme Assemblies on Electrodes

CHRISTIAN BOURDILLON,[1b] CHRISTOPHE DEMAILLE,[1a] JACQUES MOIROUX,*,[1a] AND JEAN-MICHEL SAVÉANT*,[1a]

Laboratoire d'Electrochimie Moléculaire de l'Université Denis Diderot (Paris 7), Unité Associée au CNRS No. 438, 2 place Jussieu, 75251 Paris Cedex 05, France, and Laboratoire de Technologie Enzymatique, Unité Associée au CNRS No. 1442, Université de Technologie de Compiègne, B.P. 529, 60205 Compiègne Cedex, France

Received April 22, 1996

Connecting an electrode with an enzyme is an important objective in order to translate specific chemical events taking place at the prosthetic group into electric signals or, alternatively, to place enzymatic reactions under the control of easy-to-manipulate potential or current variables. A route is thus opened to detailed investigations of the enzyme kinetics by electroanalytical techniques. Applications may concern both biosensors and preparative-scale transformations.[2,3] Only redox enzymes are amenable to electrical connection with an electrode, although other enzymes may be indirectly accessible through coupling with a connected redox enzyme. In many cases, direct electron transfer between the electrode and the prosthetic group is prevented by exceedingly large hopping distances, by improper orientation of the adsorbed enzyme, or by adsorptive denaturation. The presence of a redox mediator able to shuttle electrons between the electrode and the prosthetic group is then required. The mediator thus serves as a cosubstrate to the enzyme, replacing the natural cosubstrate. Setting the electrode potential at a value appropriate for generating the active form of the mediator thus results in an enhancement of the current which is a measure of the catalysis of the electrochemical oxidation (or reduction) of the substrate by the mediator−enzyme system. Treatments available from other types of catalysis of electrochemical reactions may thus be adapted for extracting the kinetic information from the catalytic currents.[4]

Attachment of the enzymatic catalytic systems to the electrode has obvious advantages for biosensor and synthesis applications. In this connection, entrapment in polymers or hydrogels and covalent attachment to the electrode are currently attracting active attention.[5−12]

This Account describes another type of immobilization of the enzyme on electrodes utilizing antibody−antigen binding procedures. In pioneering studies,[13] a similar immunological method was employed to immobilize enzymes on a surface. Another immunological approach was developed for enzyme-linked immunosorbent assays.[14] Avidin−biotin interaction[5d,15,16] and self-assembly of multicomponent proteins[17,18] provide alternative linking procedures that may be used for similar purposes. Whatever the attachment strategy, it is important, although very seldom achieved in current work, to ascertain the

Christian Bourdillon was born in 1945. He received his education at the University of Rouen. He partook in the creation of the Technology University of Compiègne where he is currently Professor. His current research interests involve the coupling between enzymatic technology and electrochemistry and extend to the study of biological electron carriers in supported lipid structures.

Christophe Demaille was born in 1968. He achieved his undergraduate and graduate studies at the University Denis Diderot (Paris 7). He is currently a postdoctoral fellow at the University of Texas at Austin and plans to develop in the future further enzymatic constructions on electrodes.

Jacques Moiroux was born in 1943. He received his education at the Ecole Normale Supérieure de Cachan where he taught before becoming a Professor at the University of Picardie in Amiens. He joined the University Denis Diderot (Paris 7) in 1991. His general field is bioorganic electrochemistry. His current research interests involve the reactivity of redox enzymes and the physical chemistry of the oxidation of molecules of biological interest.

Jean-Michel Savéant was born in 1933. He received his education at the Ecole Normale Supérieure in Paris where he became the Vice-Director of the Chemistry Department before moving to the University Denis Diderot (Paris 7) as a Professor in 1971. He is, since 1985, Directeur de Recherche au Centre National de la Recherche Scientifique. His current research interests involve all aspects of molecular electrochemistry, including enzymatic catalysis, as well as mechanisms and reactivity in electron transfer chemistry.

(1) (a) Université Denis Diderot. (b) Université de Technologie de Compiègne.

(2) Turner, A. P. F.; Karube, I.; Wilson, G. S. *Biosensors*; Oxford University Press: Oxford, 1987.

(3) (a) Simon, H.; Bader, J.; Gunther, H.; Neumann, S.; Thanos, J. *Angew. Chem., Int. Ed. Engl.* **1985**, *24*, 539. (b) Bourdillon, C.; Lortie, R.; Laval, J. M. *Biotechnol. Bioeng.* **1988**, *31*, 553. (c) Frede, M.; Steckhan, E. *Tetrahedron Lett.* **1991**, *32*, 5063.

(4) (a) Savéant, J.-M.; Vianello, E. In *Advances in Polarography*; Longmuir, I. S., Ed.; Pergamon Press: London, 1960; Vol. 1, pp 367−374. (b) Andrieux, C. P.; Savéant, J.-M. In *Electrochemical Reactions in Investigation of Rates and Mechanisms of Reactions, Techniques of Chemistry*; Bernasconi, C. F., Ed.; Wiley: New York, 1986; Vol. VI/4E, Part 2, pp 305−390.

(5) (a) Heller, A. *Acc. Chem. Res.* **1990**, *23*, 128. (b) Schuhmann, W.; Ohara, T. J.; Schmidt, H.-L.; Heller, A. *J. Am. Chem. Soc.* **1991**, *113*, 1394. (c) Aoki, A.; Heller, A. *J. Phys. Chem.* **1993**, *97*, 11014. (d) Vreeke, M. S.; Rocca, P.; Heller, A. *Anal. Chem.* **1995**, *67*, 303.

(6) (a) Foulds, N. C.; Lowe, C. R. *Anal. Chem.* **1988**, *60*, 2473. (b) Wolowacs, S. E.; Yon Hin, B. F. Y.; Lowe, C. R. *Anal. Chem.* **1992**, *64*, 1541.

(7) (a) Kajiya, Y.; Sugai, H.; Iwakura, C.; Yoneyama, H. *Anal. Chem.* **1991**, *63*, 49. (b) Belanger, D.; Nadreau, J.; Fortier, G. *Electroanalysis* **1992**, *4*, 933. (c) Coche-Guerente, L.; Deronzier, A.; Maillet, P.; Moutet, J. C. *Anal. Chim. Acta* **1994**, *289*, 143. (d) Wang, J.; Reviejo, A. J.; Angnes, L. *Electroanalysis* **1993**, *5*, 575.

(8) Bartlett, P. N.; Tebbut, P.; Tyrrell, C. H. *Anal. Chem.* **1992**, *64*, 138.

(9) (a) Willner, I.; Kasher, R.; Zahavy, E.; Lapidot, N. *J. Am. Chem. Soc.* **1992**, *114*, 10963. (b) Willner, I.; Lapidot, N.; Riklin, A.; Kasher, R.; Zahavy, E.; Katz, E. *J. Am. Chem. Soc.* **1994**, *116*, 1428. (c) Riklin, A.; Willner, I. *Anal. Chem.* **1995**, *67*, 4118.

(10) Bourdillon, C.; Bourgeois, J. P.; Thomas, D. *J. Am. Chem. Soc.* **1980**, *102*, 4231.

(11) Kamin, R. A.; Wilson, G. S. *Anal. Chem.* **1980**, *52*, 1198.

(12) (a) Ianiello, R. M.; Yacynych, A. M. *Anal. Chem.* **1981**, *53*, 2090. (b) Sasso, S. V.; Pierce, R. J.; Walla, R.; Yacynych, A. M. *Anal. Chem.* **1990**, *62*, 1111.

(13) (a) Lomen, C. E.; de Alwis, W. U.; Wilson, G. S. *J. Chem. Soc., Faraday Trans. 1* **1986**, *82*, 1265. (b) de Alwis, W. U.; Hill, B. S.; Meiklejohn, B. I.; Wilson, G. S. *Anal. Chem.* **1987**, *59*, 2688.

(14) (a) Robinson, G. A.; Cole, V. M.; Rattle, S. J.; Forrest, G. C. *Biosensors* **1986**, *2*, 45. (b) Gyss, C.; Bourdillon, C. *Anal. Chem.* **1987**, *59*, 2350.

S0001-4842(96)00137-9 CCC: $12.00

Scheme 1

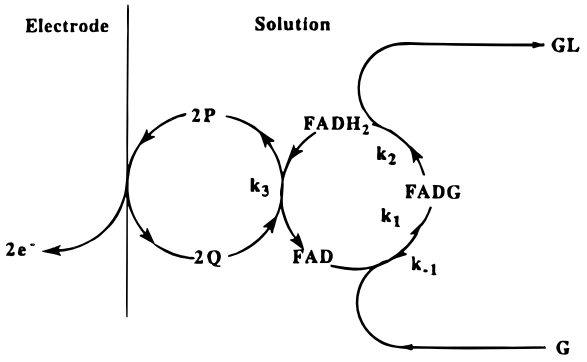

activity of the enzyme sites in the deposited layers. Particular attention is devoted to this point in the examples described in the following sections. They will also illustrate how step-by-step immunological attachment allows the construction of multilayer electrode coatings. How can it be demonstrated that such assemblies are spatially ordered? As shown below, the answer resides in the analysis of the catalytic current responses under conditions where they are jointly governed by the enzymatic reaction and by the mediator diffusion through the film. Another advantage of the step-by-step strategy is the possibility to inactivate any set of monolayers in the multilayer coating. On the whole, it is thus possible to control spatial order and enzymatic activity. Although transposable to any system involving a redox enzyme and of an electrochemically regenerable cosubstrate, the precise demonstration of the construction procedures and kinetic analyses need the examination of a specified system which may then serve as a model for future studies. This consisted of glucose oxidase and single electron acceptor mediators, mostly ferrocenes. A necessary preliminary step, in this case as in others, is that the homogeneous enzymatic kinetics should be known in sufficient detail. At this occasion, an interesting general question arose, namely, what is the extent and nature of molecular recognition between a redox enzyme and artificial one-electron cosubstrates?

One-Electron Artificial Cosubstrates in Homogeneous Reactions

The principle of homogeneous enzymatic catalysis is summarized in Scheme 1, taking as an example the catalysis of the electrochemical oxidation of β-D-glucose (G) into glucono-δ-lactone (GL) by the enzyme−mediator system (P is the reduced form of the mediator, e.g., a ferrocene, and Q its oxidized form, e.g., a ferricinium). Figure 1 represents two typical examples of cyclic voltammetric catalytic responses.[19] In the absence of enzymatic reaction, the current is governed by the diffusion of both forms of the mediator between the electrode and the bulk of the solution (as

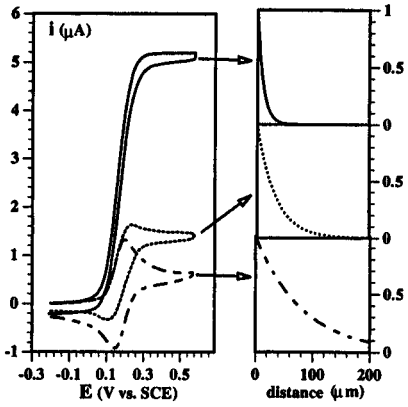

Figure 1. Glucose oxidase catalyzed electrochemical oxidation of β-D-glucose mediated by ferricinium methanol. Dashed lines: cyclic voltammograms of ferrocenemethanol (0.1 mM) in the absence or presence of glucose (0.5 M). Dotted and full lines: after addition of glucose oxidase (2.7 μM) at pH 4.5 (acetate buffer) and 6.5 (phosphate buffer), respectively. Ionic strength: 0.1 M. Scan rate: 0.08 V/s. Electrode surface area: 0.07 cm^2. Temperature: 25 °C. Panels on right: concentration profiles of the oxidized form of the mediator (Q).

seen in the lower-right panel, the thickness of the diffusion layer is on the order of 100 μm at 0.1 V/s). Upon addition of glucose oxidase and glucose, the increase of the anodic current is caused by the regeneration of P resulting from the reaction of Q with $FADH_2$ producing FAD (Scheme 1). The reaction of glucose with FAD regenerates $FADH_2$, thus closing the catalytic loop. Three phenomena control the current, namely, diffusion of the cosubstrate to and from the electrode, reaction of the substrate with the enzyme, and reaction of the cosubstrate with the enzyme. Two independent parameters are thus required to describe the overall kinetics,

$$\lambda = (2k_3[\mathrm{E}]/v)(RT/F) \quad \text{and} \quad \sigma = k_3[\mathrm{P}]/k_{\mathrm{enz}}$$

$k_{\mathrm{enz}} = k_1k_2[\mathrm{G}]/(k_1[\mathrm{G}] + k_{-1} + k_2) = k_{\mathrm{red}}K_{\mathrm{M}}[\mathrm{G}]/(K_{\mathrm{M}} + [\mathrm{G}])$ ($k_{\mathrm{red}} = k_1k_2/(k_{-1} + k_2)$, $K_{\mathrm{M}} = k_2/k_{\mathrm{red}}$, and [E], [G], and [P] are the total bulk concentrations of the enzyme (expressed as the concentration of catalytically active FAD,[20] glucose, and mediator, respectively). σ is a measure of the competition between the mediator−enzyme reaction and the glucose−enzyme reaction for the control of the catalytic process. λ measures the competition between the mediator−enzyme reaction and the mediator diffusion. If λ is small, the current response is entirely governed by mediator diffusion (dashed curve in Figure 1). Upon increasing λ, the reversibility progressively vanishes and a plateau appears on the anodic response. The plateau current is given by eq 1 (F is the Faraday constant, S the

$$\frac{i_{\mathrm{p}}}{FS} = 2\left(\frac{D[\mathrm{E}]}{\frac{1}{k_2} + \frac{1}{k_{\mathrm{red}}[\mathrm{G}]}}\right)^{1/2}[\mathrm{P}]^{1/2}\left\{1 - \frac{1}{\left(\frac{k_3}{k_2} + \frac{k_3}{k_{\mathrm{red}}[\mathrm{G}]}\right)[\mathrm{P}]}\ln\left[1 + \left(\frac{k_3}{k_2} + \frac{k_3}{k_{\mathrm{red}}[\mathrm{G}]}\right)[\mathrm{P}]\right]\right\}^{1/2} \quad (1)$$

electrode surface area, and D the diffusion coefficient of the cosubstrate). Under these conditions, the

(15) (a) Pantano, P.; Morton, T. H.; Kuhr, W. G. *J. Am. Chem. Soc.* **1991**, *113*, 1832. (b) Pantano, P.; Kuhr, W. G. *Anal. Chem.* **1993**, *65*, 623.

(16) Müller, W.; Ringsdorf, H.; Rump, E.; Wildburg, G.; Zhang, X.; Angelmaier, L.; Knoll, W.; Liley, M.; Spinke, J. *Science* **1993**, *262*, 1706.

(17) Lvov, Y.; Ariga, K.; Ichinose, I.; Kunitake, T. *J. Am. Chem. Soc.* **1995**, *117*, 6117.

(18) Mrksich, M.; Grunwell, J. R.; Whitesides, G. M. *J. Am. Chem. Soc.* **1995**, *117*, 12009.

(19) Bourdillon, C.; Demaille, C.; Moiroux, J.; Savéant, J.-M. *J. Am. Chem. Soc.* **1993**, *115*, 2.

(20) Weibel, M. K.; Bright, H. J. *J. Biol. Chem.* **1971**, *246*, 2734.

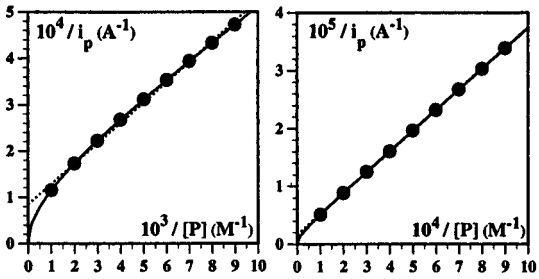

Figure 2. $1/i_p$ vs 1/[P] plots predicted by eq 2. $S = 0.2$ cm^2, $D = 6.7 \times 10^{-6}$ cm^2 s^{-1}, [E] $= 2.7 \times 10^{-6}$ M, [G] $= 0.05$ M, $k_2 = 780$ s^{-1}, $k_{red} = 1.2 \times 10^4$ M^{-1} s^{-1}, $k_3 = 6 \times 10^6$ M^{-1} s^{-1}.

diffusion and reaction of the mediator compensate each other, giving rise to a steady-state regime. Thus, the plateau current is independent of the scan rate. Upon increasing λ, the mediator concentration profile is confined within a thinner and thinner reaction layer adjacent to the electrode (upper-right and middle-right panels of Figure 1). The expression of the plateau current is then independent of the exact diffusion regime and thus of the shape of the electrode (disk, sphere, cylinder, ...). It is also valid at very low scan rates where, because of the interference of convection, the diffusion regime ceases to be semi-infinite. Equation 1 does not give rise to Lineweaver−Burk plots (eq 2) in which the plateau current would be proportional to the rate, ν, of the enzymatic reaction as is sometimes incorrectly assumed.[21]

$$\frac{1}{\nu} = \frac{1}{2k_2[\mathrm{E}]} + \frac{k_{-1} + k_2}{2k_1k_2[\mathrm{E}][\mathrm{G}]} + \frac{1}{2k_3[\mathrm{E}][\mathrm{P}]} \qquad (2)$$

The real $1/i_p$ vs 1/[P] curve goes through the origin and is not a straight line (Figure 2). The slope and intercept of the approximate straight line one may draw through experimental points do not therefore have the meaning suggested by eq 2.

The reason that homogeneous kinetics depicted by eq 2 are not directly applicable to the electrochemical data resides in the fact that the cosubstrate, Q, reacts while diffusing away from the electrode surface. Unlike oridinary homogeneous kinetics, the cosubstrate concentration is space dependent; i.e., under most practical conditions it is a function of the distance x to the electrode surface. To clarify this point, consider the simple case of a nonenzymatic reaction where a substrate, S, in excess concentration ([S]), would react with the mediator, Q, with a two-electron stoichiometry. If the rate-determining step (rate constant k) is much faster than diffusion (i.e., the competition parameter $\lambda = (RT/F)(k/v)$ is large), the current−potential curve is plateau shaped, indicating that diffusion and reaction are compensating each other. A steady-state situation is thus reached, depicted by eq 3, a combination between Fick's second

$$0 \approx \frac{\partial C_Q}{\partial t} = D\frac{\partial^2 C_Q}{\partial x^2} - 2k[\mathrm{S}]C_Q \qquad (3)$$

law describing diffusion and a homogeneous kinetic term in which the time (t) dependence of the cosubstrate concentration, C_Q, is regarded as negligible.

(21) Marx-Tibbon, S.; Katz, E.; Willner, I. *J. Am. Chem. Soc.* **1995**, *117*, 9925.

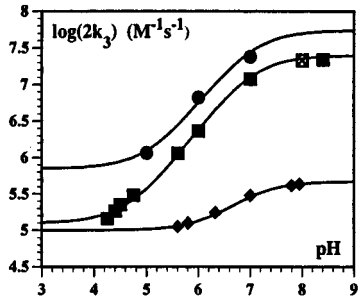

Figure 3. Catalysis of the electrochemical oxidation of glucose by glucose oxidase mediated by one-electron redox cosubstrates. Variation of the oxidation rate constant, k_3, with pH. Ionic strength: 0.1 M. Temperature: 25 °C. Native enzyme + ferricinium methanol (■), + ferricinium carboxylate (◆), + (dimethylammonio)ferricinium (●). Recombinant enzyme + ferricinium methanol (× inside □).

Integration then leads to an exponentially decreasing profile (eq 4) of the type shown in the upper-right

$$C_Q = [\mathrm{P}]\exp\left[-\left(\frac{D}{2k[\mathrm{S}]}\right)^{1/2}\right] \qquad (4)$$

panel of Figure 1, and to an expression of the diffusion flux at the electrode surface, and thus of the current, given by eq 5. Equation 1 is a slightly more compli-

$$\frac{i_p}{FS} = -D\left(\frac{\partial C_Q}{\partial x}\right)_{x=0} = (2k[\mathrm{S}]D)^{1/2}[\mathrm{P}] \qquad (5)$$

cated version of eq 5, where the concentration of the enzyme and the three rate characteristic constants of the enzymatic reaction appear and where the log term results from the integration of the enzymatic reaction kinetics over the reaction layer in an equation similar to eq 4.

When σ is small, an asymptotic first-order kinetics is followed corresponding to eq 6. this behavior can be obtained when [P] is small enough but also when $k_3[(1/k_2) + (1/k_{red}[\mathrm{G}])]$ is small. Depending on the

$$\frac{i_p}{FS} = (2D[\mathrm{E}]k_3)^{1/2}[\mathrm{P}] \qquad (6)$$

value of k_3/k_2, increasing the glucose concentration may not be sufficient to reach the first-order behavior. Under such conditions, forced application of eq 6 leads to erroneous values of k_3.[22]

Coming back to the experiments shown in Figure 1, we note that the thickness of the thinnest reaction layer is on the order of 20 μm. It is therefore *ca.* 2000 times the size of the enzyme. These are typical orders of magnitude, pointing to the general conclusion that the kinetics derived from the above procedures concern enzymes dispersed in the solution and not a layer of adsorbed enzyme.

As with many redox enzymes, the prosthetic group does not merely exchange electrons with the cosubstrate but electrons and protons. Analysis of the variation of k_3 with pH by means (Figure 3) of eq 1 is thus an example of the general procedures that may be followed to uncover the role of protons. The redox and proton transfer reactions undergone by the flavin

(22) Cass, A. E. G.; Davis, G.; Francis, G. D.; Hill, H. A. O.; Aston, W. J.; Higgins, I. J.; Plotkin, E. V.; Scott, L. D. L.; Turner, A. P. F. *Anal. Chem.* **1984**, *56*, 667.

Scheme 2

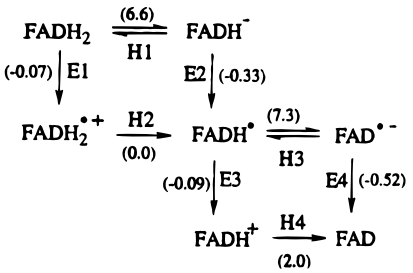

Table 1. Characteristic Rate Constants of Glucose Oxidation by Glucose Oxidase Immobilized on the Glassy Carbon Electrode by Antibody−Antigen Attachment

enzyme	immobilized monolayer[30]	in solution	
mediator	ferrocene-methanol	ferrocene-methanol[19]	O_2[20]
k_3 (M^{-1} s^{-1})	$(1.3 \pm 0.3) \times 10^7$	$(1.2 \pm 0.1) \times 10^7$	
k_2 (s^{-1})	600 ± 200	680 ± 100	750
k_{red} (M^{-1} s^{-1})	$(0.9 \pm 0.3) \times 10^4$	$(1.1 \pm 0.2) \times 10^4$	1.1×10^4

prosthetic group are summarized in Scheme 2. The vertical reactions are oxidations by Q regenerating P. From the values (V vs SCE) of the standard potentials of the four flavin redox couples[23] which are involved in Scheme 2 and those of the mediators (Table 1), all four oxidation steps may be regarded as irreversible. The horizontal reactions are deprotonations by the bases present in the buffer. From the pK_a values of the various flavin acid−base couples indicated in Scheme 2 (over or below the horizontal arrows),[23] reactions H2 and H4 may be regarded as irreversible and reactions H1 and H3 as reversible in the pH range of interest (4−8.5). Experiments where the concentration of the buffer was varied showed that reactions H1 and H3 remain at equilibrium. The rate constant k_3 is thus related to the various steps of Scheme 2 according to eq 7.

$$\frac{1}{k_3} = \frac{1 + \dfrac{K_{a,H1}}{[H^+]}}{k_{E1} + \dfrac{K_{a,H1}}{[H^+]}k_{E2}} + \frac{1 + \dfrac{K_{a,H3}}{[H^+]}}{k_{E3} + \dfrac{K_{a,H3}}{[H^+]}k_{E4}} \qquad (7)$$

Fitting of the data points with eq 7 leads to the sigmoid lines in Figure 3. The two limiting values of k_3, in acid and basic media, k_{ac} and k_{bas}, respectively, depend on the individual rate constants according to eq 8.

$$\frac{1}{k_{ac}} = \frac{1}{k_{E1}} + \frac{1}{k_{E3}} \qquad \frac{1}{k_{bas}} = \frac{1}{k_{E2}} + \frac{1}{k_{E4}} \qquad (8)$$

This detailed kinetic analysis is typical of the procedures to be followed to dissect a $-2e^- - 2H^+$ global reaction into its electron and proton transfer elementary steps. In the present case the electron transfer steps are rate determining. A striking observation, which may be of general interest for the reactions of oxidases, is that, thanks to the use of the artificial cosubstrates, the maximal activity of the flavin enzyme is reached above pH 8 whereas it appears around pH 5.5 with dioxygen.[20]

Further insights into the artificial cosubstrates toward the various forms of the prosthetic group are provided by a comparison of the rate constants with the driving forces (see Table 1 in ref 24). There is no parallelism between the kinetics and the driving forces such as the one predicted by a Marcus-type relationship (the larger the driving force the faster the reaction).[25] In an acidic medium, where $FADH_2$ reacts under its neutral form, the rate constant is almost independent of the driving force. In a basic medium, where the reacting species is $FADH^-$, the same lack of correlation is observed. The neutral ferricinium carboxylate reacts with approximately the same rate constant as in an acidic medium. In contrast, the positively charged ferricinium methanol and [(dimethylamino)methyl]ferricinium react about 100 times faster than in an acidic medium. In all cases, the rate constant is much below the diffusion limit (5×10^8 M^{-1} s^{-1}). In this connection, it is interesting to note that the data point for the hyperglycosylated recombinant enzyme (60−70% carbohydrate content vs 16% for the native enzyme)[26] in Figure 3 falls on the same line as the data points for the native enzyme, showing that transport through the glycoside shell around the protein core of the enzyme is also fast.

The X-ray crystal structure of glucose oxidase[27] shows that the flavin sits at the bottom of a funnel-shaped pocket with an opening of *ca.* 10 Å diameter at the surface of the proteinic core and a depth of *ca.* 10 Å. The ferricinium cosubstrates may thus experience some difficulty reaching a position geometrically suitable for efficient electron transfer. Combination of the kinetic and structural observations suggests a mechanism in which any of the four electron transfers may be decomposed into three successive steps, diffusion of Q toward the opening of the pocket at the surface of the protein core of the enzyme, displacement toward the flavin in a position geometrically suited for electron transfer, and electron transfer.[24] Each of the electron transfer steps is controlled neither by the rate of electron transfer nor by the diffusive approach of the one-electron cosubstrate toward the opening of the pocket at the surface of the protein core of the enzyme. The rate-determining factor appears to be the sterically hindered positioning appropriate for electron transfer to occur. The kinetics thus reveals some molecular recognition between the artificial one-electron cosubstrates by the enzyme. Recent experiments, using the two enantiomers of protonated *N*,*N*-dimethyl-1-ferrocenylethylamine, reported a significant chiroselectivity of the reaction,[21] implying a very precise molecular recognition. However, further attempts to reproduce these results were unsuccessful,

(23) (a) Williams, R. F.; Bruice, T. C. *J. Am. Chem. Soc.* **1976**, *98*, 7752. (b) Williams, R. F.; Shinkai, S. S.; Bruice, T. C. *J. Am. Chem. Soc.* **1977**, *99*, 921. (c) Eberlein, G.; Bruice, T. C. *J. Am. Chem. Soc.* **1982**, *104*, 1449. (d) Stankovich, M. T.; Shopfer, L. M.; Massey, V. *J. Biol. Chem.* **1978**, *253*, 4971. (e) Ghisla, S.; Massey, V. *Eur. J. Biochem.* **1989**, *181*, 1.

(24) Alzari, P.; Anicet, N.; Bourdillon, C.; Moiroux, J.; Savéant, J.-M. *J. Am. Chem. Soc.* **1996**, *118*, 6788.

(25) (a) Marcus, R. A.; Sutin, N. *Biophys. Biochim. Acta* **1985**, *811*, 265. (b) Savéant, J.-M. Single Electron Transfer and Nucleophilic Substitution. In *Advances in Physical Organic Chemistry*; Bethel, D., Ed.; Academic Press: New York, 1990; Vol. 26, pp 1−130.

(26) De Baetselier, A.; Vasavada, A.; Dohet, P.; Ha-Thi, V.; De Beukelaer, M.; Erpicum, T.; De Clerck, L.; Hanotier, J.; Rosenberg, S. *Biotechnology* **1991**, *9*, 559.

(27) Hecht, H. J.; Kalisz, H. M.; Hendle, J.; Schmid, R. D.; Schomburg, D. *J. Mol. Biol.* **1993**, *229*, 153.

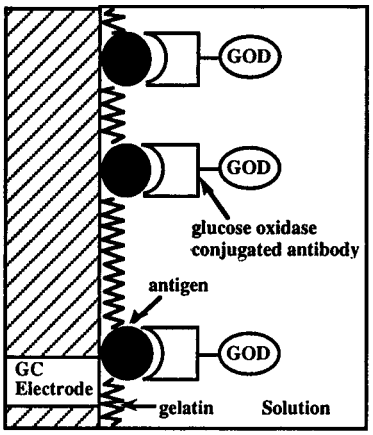

Figure 4. Sketch of the monolayer glucose oxidase electrode obtained by adsorption of rabbit IgG (antigen) and reaction with a glucose oxidase conjugated antibody, the anti-rabbit IgG (whole molecule) produced in goats. Reprinted with permission from ref 30. Copyright 1993 American Chemical Society.

the two enantiomers giving rise to the same catalytic response within experimental uncertainty.[24] Thus, molecular recognition is not precise enough to allow chiroselective electron transfer. Molecular recognition rather works in a rejection mode: steric hindrance in the pocket connecting the prosthetic group to the enzyme surface slows electron transfer, offering some resistance against a largely favorable driving force. The resulting rate constants nevertheless remain large, allowing ferricinium ions to act as quite efficient cosubstrates. It would be interesting to test the generality of such behavior of redox enzymes toward artificial cosubstrates.

It seems worth emphasizing that electrochemical techniques, such as cyclic voltammetry, allow the use of a large variety of artificial cosubstrates, since, unlike stop-flow techniques, the active form of the cosubstrate need not to be chemically stable. It suffices that the cosubstrate reacts with enzyme faster than any other species present in the solution.

Antibody−Antigen Construction of Monolayer Coatings. Reactivity Characterization

Adsorption of the enzyme on a glassy carbon electrode does not produce any catalytic current. Either adsorption is too weak or it denaturates the enzyme, as it does on platinum.[28] Chemical immobilization techniques[10,12,29] also suffer the danger of enzyme denaturation.

The immunological attachment technique described below was developed for minimizing denaturation. The electrode, prepared by the antigen−antibody technique, is sketched in Figure 4.[30] Adsorption of rabbit IgG is followed by adsorption of gelatin and specific binding of a glucose oxidase conjugated antibody.

Cyclic voltammetry allows a precise kinetic characterization of such systems starting from the observation of catalytic responses (Figure 5). The characteristic rate constants are derived from the catalytic

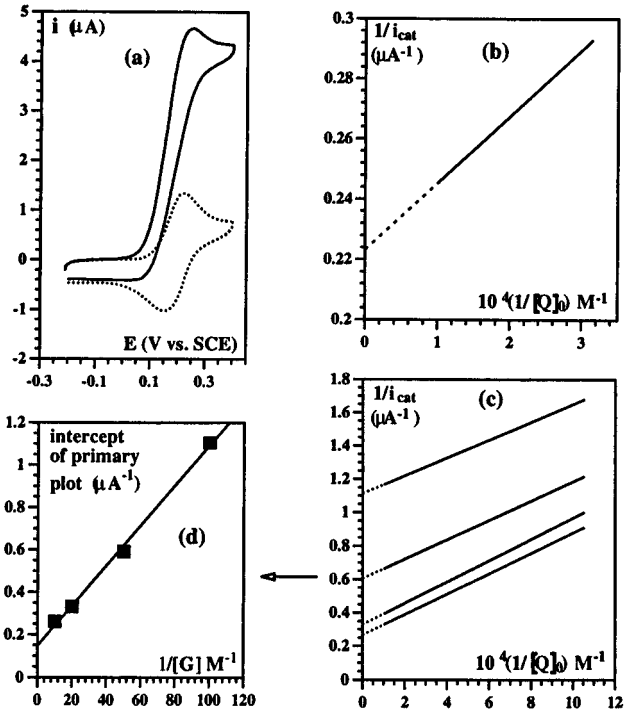

Figure 5. Antigen−antibody immobilized glucose oxidase GC electrode. Temperature: 25 °C. (a) Cyclic voltammetry at saturation coverage of the enzyme with a 0.1 M glucose concentration and ferrocenemethanol (0.1 mM) as mediator in a pH 8 phosphate buffer (0.1 M ionic strength). The dotted and solid lines represent the cyclic voltammogram (0.04 V/s) in the absence and presence of glucose (0.1 M), respectively. (b) Primary plot obtained at saturation coverage of the enzyme with a 0.01 M glucose concentration. (c) Primary plots obtained with a partial (37%) enzyme coverage for (from top to bottom) 0.01, 0.2, 0.05, and 0.1 M glucose. (d) Secondary plot derived from the intercepts of the primary plots in (c).

current, i_{cat}, by application of eq 9,[30] where Γ_E^0 is the

$$\frac{1}{i_{cat}} = \frac{1}{2Fk_3\Gamma_E^0}\frac{1}{(C_Q)_0} + \frac{1}{2F\Gamma_E^0}\left(\frac{1}{k_2} + \frac{1}{k_{red}[G]}\right) \quad (9)$$

amount of immobilized active enzyme and $(C_Q)_0$ the concentration of the oxidized form of the cosubstrate at the electrode surface (eq 10). Primary and second-

$$(C_Q)_0 = \frac{[P]}{1 + \exp\left[-\frac{F}{RT}(E - E_{QP}^0)\right]} \quad (10)$$

ary plots ensue (Figure 5), leading to the characteristic rate constants. This derivation however requires the value of the surface concentration of active enzyme, Γ_E^0. Radioactive ^{125}I labeling affords the total amount of enzyme, active and inactive, present on the electrode surface.[30] If one uses the values of Γ_E^0 thus obtained, assuming that all the enzyme is active, the rate constant values listed in Table 1 ensue. They are the same as obtained previously in homogeneous experiments, indicating that the enzyme deposited on the electrode surface is fully active. The stability of the electrode response was found to be good (0.3% decay per day). It is remarkable that the stability of the enzyme is significantly better in the film than in solution (by a factor of about 20), presumably due to the high local concentration of proteins (190 mg/mL) around the enzyme sites.

(28) Szucs, A.; Hitchens, G. D.; Bockris, J. O. *J. Electrochem. Soc.* **1989**, *136*, 3748.
(29) Bourdillon, C.; Delamar, M.; Demaille, C.; Hitmi, R.; Moiroux, J.; Pinson, J. *J. Electroanal. Chem.* **1992**, *336*, 113.
(30) Bourdillon, C.; Demaille, C.; Guéris, J.; Moiroux, J.; Savéant, J.-M. *J. Am. Chem. Soc.* **1993**, *115*, 12264.

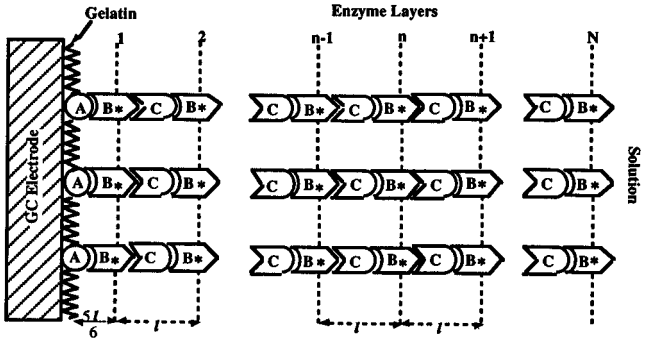

Figure 6. Sketch of the *N* monolayers of glucose oxidase film on a glassy carbon electrode surface: (A) adsorbed mouse IgG (antigen), (B) anti-mouse IgG glucose oxidase conjugate (antibody), (C) monoclonal antibody to glucose oxidase produced in mice. An asterisk indicates the approximate location of a glucose oxidase moiety.

These results show that, unlike adsorptive and chemical techniques, the immunological approach to the grafting of the electrode surface preserves the activity of the enzyme quite efficiently.

Step-by-Step Construction of Multilayer Coatings. Spatial Order

The step-by-step immunological construction of a set of enzyme monolayers is sketched in Figure 6.[31] In the example shown, the attachment of a second monolayer requires a monoclonal antibody to glucose oxidase (C). At one end, C binds to the enzyme contained in B. At the other it serves as an antigen for B. It is thus possible to attach a second monolayer to the first, a third to the second, and so on (Figure 6).

Figure 7a shows a typical example of the increase of the catalytic response upon increasing the number of monolayers deposited on the electrode. The plateau current, i_p, is given by eq 11 when the catalytic

$$\frac{1}{i_p} = \frac{1}{2F\Gamma_E}\left(\frac{1}{k_3\kappa_Q[P]} + \frac{1}{k_2} + \frac{1}{k_{red}\kappa_G[G]}\right) \qquad (11)$$

reaction is rate controlling. κ_G and κ_Q are the partition coefficients of the subscript species. Γ_E is the total amount of active enzyme in the coating. The values of the plateau current at a relatively high concentration of cosubstrate, 0.2 mM, are proportional to the number of enzyme monolayers deposited, with only a slight downward deviation for the 9th and 10th layers (Figure 7b). In the linear region of the diagram, $\Gamma_E = N\Gamma_E^0$; i.e., each monolayer contains the same amount of active enzyme. Downward deviation from proportionality increases as the concentration of cosubstrate decreases (Figure 7b), reflecting the increasing interference of cosubstrate mass transport through the film. The rate of diffusion of the cosubstrate through the film increases proportionally to [P]. The rate of the catalytic reaction also increases with [P] but less than proportionally (Figure 7c). Upon increasing [P], a situation is thus reached where the catalytic reaction becomes rate-determining. A second factor of the competition is the thickness of the film. As it increases upon depositing more and more enzyme layers,

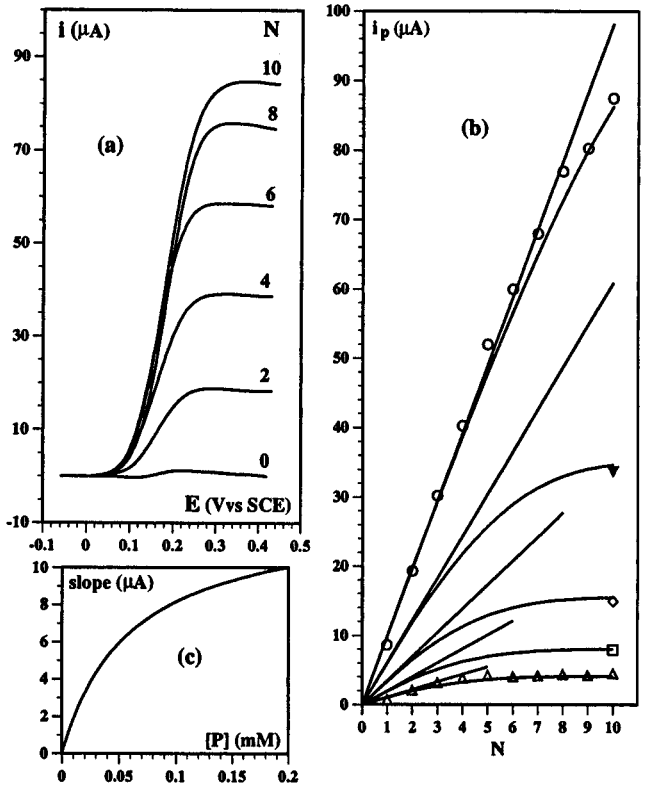

Figure 7. Cyclic voltammetry of glucose oxidase coated GC electrodes with an increasing number (*N*) of monolayers in a pH 8 phosphate buffer (ionic strength 0.1 M) solution containing 0.5 M glucose. Scan rate: 0.04 V/s. Temperature: 25 °C. (a) Voltammograms for 0.2 mM ferrocenemethanol mediator; from bottom to top, $N = 0$, 2, 4, 6, 8, and 10 (for clarity the odd numbers of monolayer are not represented). (b) Plateau currents as a function of *N* for several concentrations of the ferrocenemethanol mediator: 0.2 (○), 0.05 (▼), 0.02 (◇), 0.01 (□), 0.005 (△). Straight lines: linear responses corresponding to $\Gamma_E^0 = 10^{-12}$ mol, $k_3 = 1.2 \times 10^7$ M^{-1} s^{-1}, $k_2 = 700$ s^{-1}, $k_{red} = 10^4$ M^{-1} s^{-1}. Curved lines: simulation of the interference of mediator mass transport. (c) Slope of the straight lines in (b) as a function of the cosubstrate concentration.

diffusion of the cosubstrate slows and tends to become rate-determining (Figure 7b).

Application of eq 11 to the linear portions of the $i_p - N$ plots in Figure 7b shows that $\kappa_Q = 1$. At a low scan rate, e.g., 0.1 V/s, the thickness of the cosubstrate diffusion layer is on the order of 200 μm. The thickness of the thicker enzyme films ($N = 12$) is much smaller, on the order of 0.6 μm. Thus, in the absence of substrate, the cyclic voltammetric response of an enzyme-coated electrode simply reflects the diffusion of the cosubstrate in the solution with a standard potential of

$$E_{Q/P}^{0'} = E_{Q/P}^0 + (RT/F)\ln(\kappa_P/\kappa_Q)$$

Experiments carried out at 0.1 V/s showed that $E_{Q/P}^{0'} = E_{Q/P}^0$ and thus that $\kappa_P = \kappa_Q = 1$.[31b] Upon raising the scan rate to 20 V/s, the diffusion layer thickness, 10^{-4} cm, becomes the same order of magnitude as that of the thicker enzyme films. The voltammetric responses thus become sensitive to the diffusion of the cosubstrate through the film. It was thus found that $D_P/D = 0.6$ and $D_Q/D = 1$[31b] (D_P and D_Q are the diffusion coefficients of the reduced and oxidized forms of the cosubstrate within the film, and *D* is the common

(31) (a) Bourdillon, C.; Demaille, C.; Moiroux, J.; Savéant, J.-M. *J. Am. Chem. Soc.* **1994**, *116*, 10328. (b) Bourdillon, C.; Demaille, C.; Moiroux, J.; Savéant, J.-M. *J. Am. Chem. Soc.* **1995**, *117*, 11499.

value of the diffusion coefficients of the reduced and oxidized forms of the cosubstrate in the solution).

Knowing the parameters of the mass transport of the cosubstrate through the film, one can simulate[31b] the plateau current as a function of the number of enzyme monolayers and of the cosubstrate concentration. The only adjustable parameter is then the thickness of one monolayer, l (Figure 6). The fit displayed in Figure 7b corresponds to $l = 475$ Å, a quite reasonable value from what is known about the size of the proteins involved.[28]

Once built, a film containing any number of monolayers, $N - 1$, can be deactivated with iodoacetate under cyclic voltammetric monitoring. After complete deactivation, an active Nth layer can be grafted on top of the $N - 1$ inactive layers. This procedure leads to a surface concentration of enzyme in the Nth layer which is 60−80% of Γ_E^0, the surface concentration of enzyme per active layer. However, when a $(N + 1)$th active layer is deposited, the surface concentration again reaches Γ_E^0. The same is true for all active layers that can be successively deposited. These results indicate that 20−40% of the enzymes are affected by the chemical deactivation in a way that hampers their recognition by the monoclonal antibodies to glucose oxidase which allows the attachment of the Nth layer. This deficit is however canceled when the $(N + 1)$th layer is grafted since each of the two monoclonal antibodies used in the experiments can recognize two separated peripheric epitopes of the same glucose oxidase unit.

The analysis of the catalytic responses of such partially deactivated films allows the testing of the spatial order resulting from the antigen−antibody construction method. Two such films were tested. For example, one was made of 10 inactivated monolayers on top of which one active monolayer was grafted. The plateau currents obtained at three cosubstrate concentrations, 0.4, 0.02, and 0.01 mM, could be satisfactorily simulated, as resulting from the combined effect of cosubstrate diffusion and enzymatic reaction, using the same parameters as above, notably the same value for the thickness of one monolayer.[31b] The same result was obtained with films made of five inactivated monolayers followed by one, two, three, four, and five active monolayers.[31b]

We may thus conclude that Figure 6 is not merely a pictorial representation of the grafting of successive monolayers of enzyme but represents a real spatial order induced by the antigen−antibody interactions, the templating effect of the electrode surface, and the self-optimization of the lateral compactness of each monolayer.

Conclusions and Perspectives

Starting with a sacrificial antigen adsorbed on the electrode surface which is then combined with the enzyme-conjugated antibody, it is possible to build a fully active enzyme monolayer. The method can be extended to the step-by-step deposition of any number of enzyme monolayers using a monoclonal antibody to the enzyme as an immunological link between two successive monolayers. Inactivation of a first series of monolayers followed by the grafting of one or more active monolayers allows the construction of a large variety of systems where activity and spatial order are precisely controlled. Cyclic voltammetry appears as a particularly convenient tool for investigating the electron transfer connection between the electrode and the prosthetic groups of the enzymatic system by means of simple one-electron mediators acting as cosubstrate to the enzyme. It also allows the precise kinetic characterization of the enzyme coatings. The systematic application of the theory of catalytic currents affords the various rate constants of the enzymatic reaction and demonstrates the interference of the mass transport of the substrate and of the cosubstrate through the film. This strategy, combined with the radioactive labeling of the enzyme, allows the demonstration that the immunological construction of the coatings preserves the activity of the enzyme units. It also establishes the existence of a spatial order of the enzymatic system induced by the antigen−antibody interactions, the templating effect of the electrode surface, and the self-optimization of the lateral compactness of each monolayer. Likewise, the same type of detailed kinetic analyses reveal that the intimate mechanism of the electron transfer between artificial one-electron cosubstrates and the enzyme involves a molecular recognition process working in a mild rejection mode.

A desirable extension of the antigen−antibody construction method is the fixation of the cosubstrate which, although attached to the structure, should remain mobile enough to efficiently shuttle electrons between the electrode and the enzyme prosthetic group. The strategies for immunological immobilization and for the electrochemical characterization of the resulting systems illustrated here with the example of glucose oxidase are potentially applicable to other enzymes. Such applications concern redox enzymes but could also be extended to multienzymatic systems in which a redox enzyme would be coupled through substrates or products to an enzyme or several enzymes of a different type.

We are indebted to Dr. Jean Guéris and to Mrs. Anne-Marie Graulet (Laboratoire d'Immunoanalyse et Techniques Associées de l'Hopital Lariboisière) for their help in the ^{125}I labeling experiments, to Nathalie Anicet for a series of experiments on enantiomeric cosubstrates, and to Dr. Pedro Alzari (Laboratoire de Technologie Enzymatique de l'Uiversité de Technologie de Compiègne) for helpful discussions.

AR960137N